Radio Science, Volume 18, Number 6, Pages 801-814, November-December 1983

Controlled stimulation of VLF emissions from Siple Station, Antarctica

R. A. Helliwell

Space, Telecommunications, and Radioscience Laboratory, Stanford University, Stanford, California 94305

(Received September 20, 1982; accepted April 20, 1983.)

Coherent VLF (1.8–7 kHz) signals injected into the magnetosphere from Siple Station (L = 4.2), Antarctica, are amplified (30 dB) and trigger intense, narrowband whistler mode emissions. The mechanism of growth is believed to be wave-induced phase bunching of cyclotron resonant electrons in an interaction region near the equatorial region. A key parameter in these experiments is the spectral purity of the transmitted signal. If the width of the signal spectrum exceeds $\sim$ 10 Hz, there is significant loss of gain. In one experiment ($f \approx 3$ kHz), two equal-amplitude signals are transmitted with a frequency spectrum of Δf. When $\Delta f = 20$ Hz, the gain is reduced as much as 20 dB below its single-frequency value. For $f \geq 100$ Hz, the two signals tend to behave independently of one another, indicating that they interact with different electron populations. Other effects of interest include entrainment of strong free-running emissions by a relatively weak Siple signal and the frequent generation of sidebands (2–100 Hz) on Siple signals that have reached saturation. Future work at Siple Station will emphasize frequencies below 4 kHz in order to raise the energies (to >10 keV) of the precipitating electrons and hence make them more readily detectable by ground-based techniques. To achieve this goal, the dipole length will be doubled (to 43 km), which is expected to increase the maximum radiated power at 2.5 kHz by 7 dB. Later, it is planned to install a circularly polarized crossed dipole that will double the effective radiated power and permit new experiments on the polarization properties of the ionosphere and magnetosphere at VLF.

1. INTRODUCTION

This paper reviews active VLF experiments at Siple Station and reports new findings on the role of wave coherence using the new two-frequency transmissions. The nature of the experiments is illustrated in Figure 1. Signals transmitted from Siple Station enter the ionosphere where they may become trapped in one or more field-aligned ducts of enhanced ionization. Upon reaching the opposite hemisphere some of the energy may be reflected back into one or more ducts and some may exit into the earth-ionosphere waveguide to be received at Siple's conjugate point, Roberval, Quebec.

As the ducted waves cross the magnetic equator, they interact with counter-streaming energetic electrons through cyclotron resonance. The wave magnetic field perturbs these electrons in two important ways. The first is pitch angle scattering [Kennel and Petschek, 1966], in which some electrons precipitate into the ionosphere where they generate X-rays [Rosenberg et al., 1971], ionization enhancements [Helliwell et al., 1973], and light [Helliwell et al., 1980a]. The second is phase bunching of the interacting electrons [Helliwell and Inan, 1982, and references therein]. The result is amplification of the applied signal by 30 dB or more and triggering of VLF emissions. An outstanding feature of the stimulated radiation is its narrowband character (bandwidth $\approx$ 1 Hz for phase-locked growth). Accordingly, the term 'coherent wave instability' (CWI) is used to describe the interaction.

The primary purpose of Siple Station is to perform active experiments on VLF wave-particle interactions [Helliwell and Katsufrakis, 1978]. An important part of the program is the observation and interpretation of various VLF wave phenomena, including whistlers, chorus and hiss [Park and Carpenter, 1978]. Related programs at Siple Station include riometer [Rosenberg and Barcus, 1978], geomagnetic pulsations [Lanzerotti, 1978], ULF waves Arnoldy et al., 1981], photometer [Mende et al., 1980], and balloons and rockets [Matthews, 1981], as shown in the sketch of Figure 2. Recently a digital ionosonde was placed in operation at Siple. All are coordinated in a program aimed at describing the behavior of the magnetosphere-ionosphere system and understanding its role in the generation of waves and wave-particle interactions.

Paper number 3S0637.
0048-6604/83/0910-0637$08.00

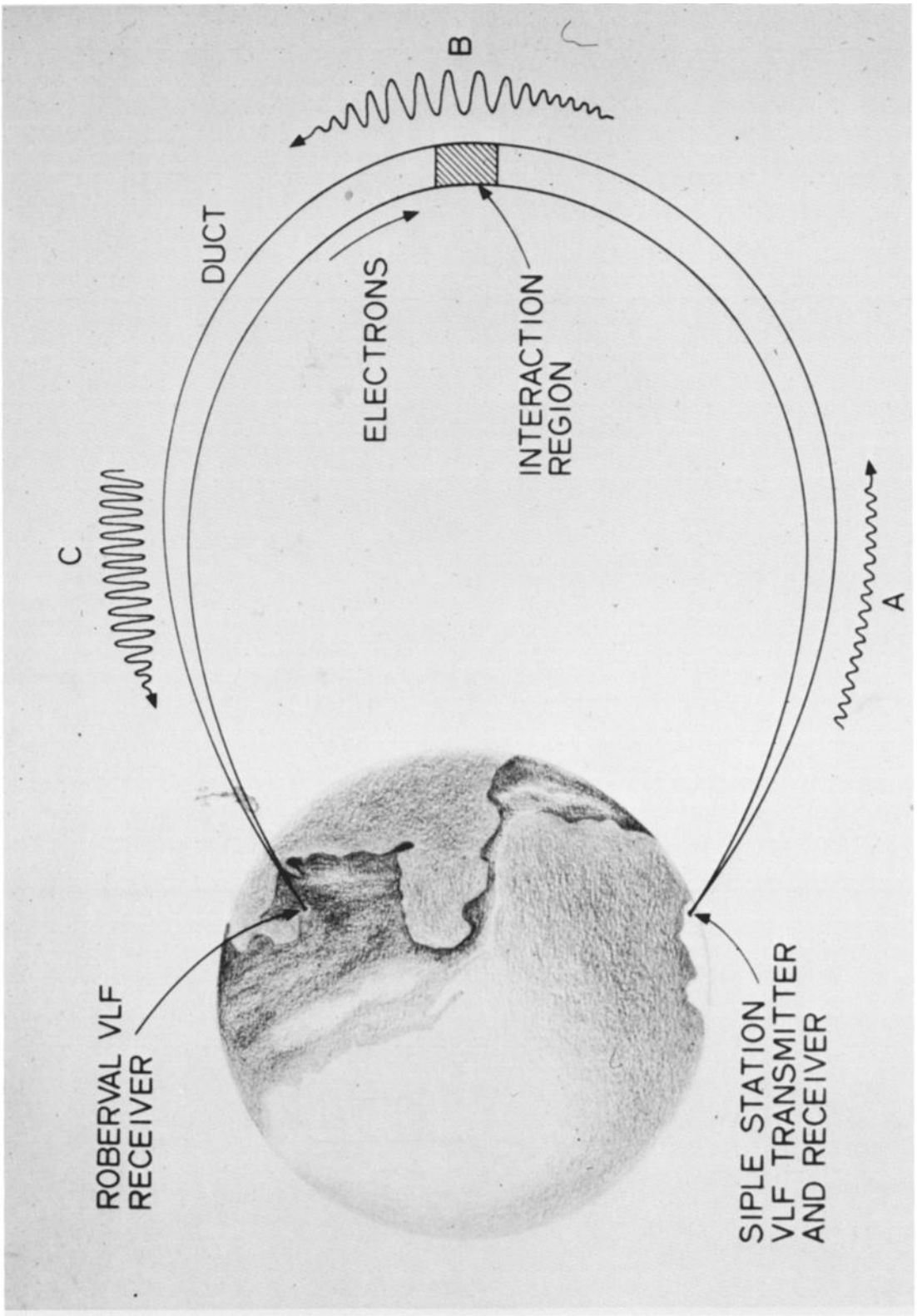

Figure 1. Sketch of field-aligned duct connecting Siple Station, Antarctica, to its conjugate point, Roberval, Quebec. Coherent signals, trapped in the duct, are amplified through cyclotron resonance with electrons in an interaction region centered on the magnetic equator.

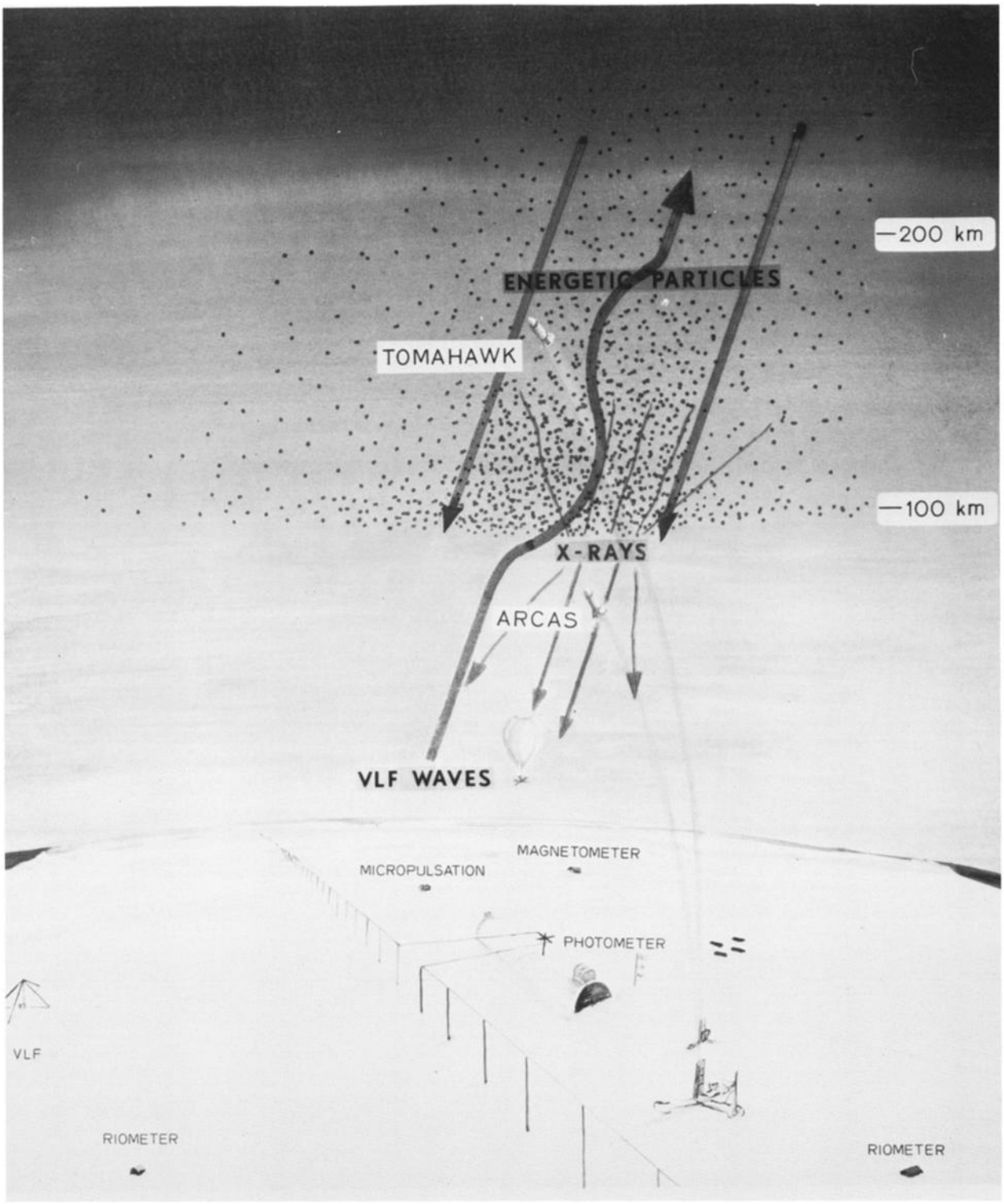

Figure 2. Sketch of Siple Station, showing VLF dipole transmitting antenna and related experiments.

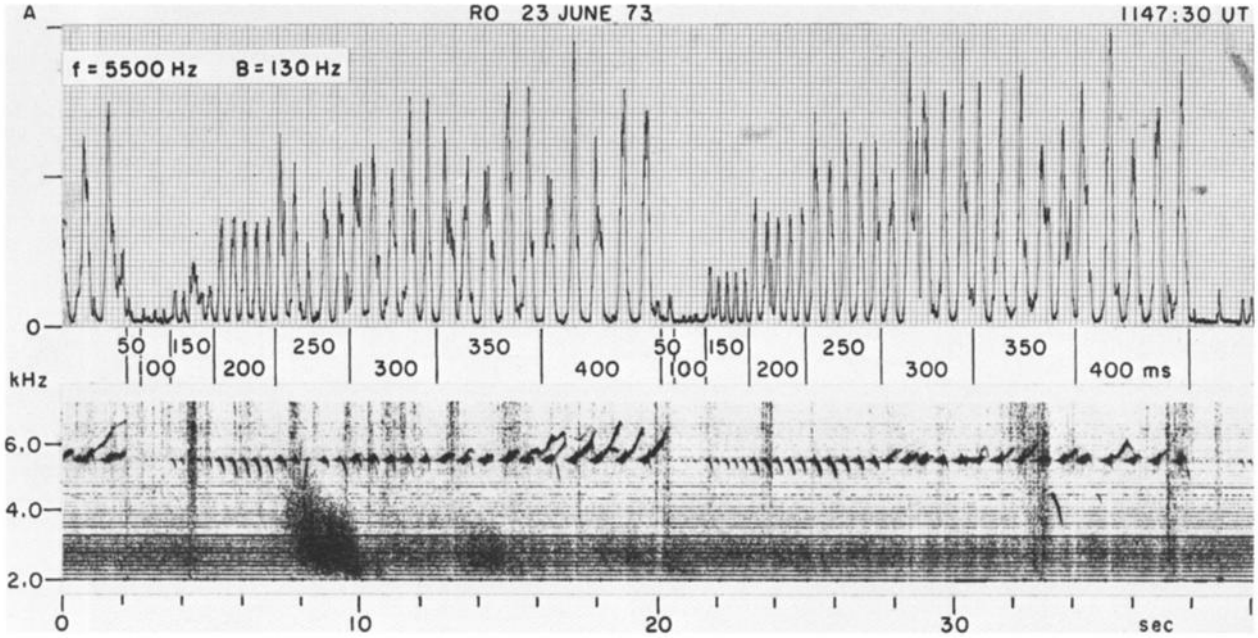

Figure 3. Response of magnetosphere to two identical sequences of coherent pulses varying in duration from 50 to 400 ms. Dynamic spectrum in lower panel shows fallers triggered at ends of shorter (≤ 250 ms) pulses and risers triggered prior to termination of longer (≤ 300 ms) pulses. Two-hop whistler at 8 s suppresses growth of third 250-ms pulse. Upper panel shows relative amplitude of received signals in a 130-Hz band centered on the carrier at 5500 Hz [after Helliwell and Katsufrakis, 1978].

The location of Siple Station was selected to satisfy the following requirements: (1) a location near the average position ($L \approx 4$) of the plasmapause, (2) a cost-effective radiator, and (3) an accessible conjugate point (Roberval, Quebec). The 2-km-thick ice sheet beneath Siple Station acts as a relatively low loss support for the 21-km-long dipole transmitting antenna. If the ice layer were not present (i.e., the dipole was erected over ordinary ground), it has been estimated that at 6 kHz the efficiency would be reduced by a factor of over 50 [Raghuram et al., 1974]. Other advantages of Siple Station include relatively low local noise levels (no thunderstorms in Antarctica), and a large number of lightning sources in the north to provide one-hop whistlers at Siple for useful diagnostic purposes.

In the next section (2) results on wave injection at a single frequency are reviewed and then in section 3 some new results from recent multifrequency experiments are introduced. In section 4 a feedback model of wave growth is reviewed and compared with available data. Finally, in section 5, a short discussion and some conclusions are presented.

2. REVIEW OF SIPLE RESULTS

An important property of wave-particle interactions at very low frequencies is coherence. The response of the magnetosphere to a coherent input signal is illustrated in Figure 3. Pulses ranging in length from 50 to 400 ms are transmitted in groups of five with a 50% duty cycle in each case. For the shorter pulses (50 and 100 ms), the response of the magnetosphere is very low, as the figures show. With each 50-ms extension in the length of the applied pulse, there is ~ 6 dB of additional growth. Saturation is reached at pulse lengths of $\sim$ 250 or 300 ms. Individual pulses show pure exponential growth as a function of time t so that the output field is given by $B = B_0 \epsilon^{\gamma t}$ where B_0 is the input signal level and γ is the growth rate. Total growth is typically 30 dB, while the growth rate ranges from 25 to 250 dB/s inside the plasmasphere [Stiles and Helliwell, 1977]. As will be shown later, growth depends on the coherence of the input signal. If the signal bandwidth exceeds ~ 10 Hz, the growth is greatly reduced.

Closely related to wave growth is the triggering of emissions. As shown in Figure 3, emissions of falling or rising frequency accompany all pulses that show growth (duration $\geq$ 100 ms). For pulse lengths exceeding 250 ms, emissions are triggered before the end of the pulse. These are called pretermination emissions. Emissions seldom cross their parent signal. Thus, for a continuous exciting wave, virtually all emissions appear only above the signal frequency.

Suppression of growth by another signal is illustrated in

Figure 3 on the third pulse of the first 250-ms sequence ($t \approx 8$ s). As can be seen from the dynamic spectrum, the reduced amplitude coincides with the appearance of a whistler component near the beginning of the Siple pulse. The effect of the superposition of these two signals is to create a spread spectrum which then reduces the growth. It is understandable therefore that Siple signals show little or no growth when there are many whistlers and/or emissions present. Unless a suitable area in frequency-time space is available, the input signal will not grow. Thus, in order for an injected signal to compete with strong natural signals, it is necessary for the injected signal to have sufficient intensity to cause suppression of the natural signals, thereby creating a clear space in the frequency-time domain. Other examples of suppression of growth can also be seen in Figure 3 where triggered emissions approach the next signal on the frequency-time plane. Delayed suppression of natural hiss by Siple signals has also been observed [Raghuram et al., 1977]. This suppression occurs in a band 50–200 Hz wide and has been called the 'quiet band effect.' It could be the result of integration of the type of suppression described above.

As Figure 3 shows, there was little detectable output from the magnetosphere until after the transmitter was turned on. This raises the question of the threshold power required for initiating the coherent wave instability. An experiment to demonstrate the behavior of the magnetosphere in response to variable input power is illustrated in Figure 4 [Helliwell et al., 1980b]. Here the pulse program consisted of constant-frequency pulses and frequency ramps as shown in the bottom panel of Figure 4b. For the maximum power input to the antenna of 24 kW (panel (a)), there are at least four paths showing growth and triggering. As the power input was reduced, in steps of 4 dB, successive repetitions of the experiment showed reduction in the number of paths, growth, and triggering, as illustrated in Figure 4b. For example, at 1.5 kW, only one path showed significant growth and triggering. At 0.6 kW that same path showed no evidence of growth or triggering. Therefore, the threshold power P_t for that path lay between 0.6 and 1.5 kW. Thus it appears that the value of P_t for each individual path is different, probably depending upon the location of the path endpoint with respect to the transmitter, as well as the flux of energetic electrons in the duct.

The sharp change in peak power output as the threshold is crossed is illustrated in Figure 4a, where the relative peak received signal in decibels is plotted as a function of the input power in decibels relative to 100 W. As can be seen from the figure, the change in output power as P_t was crossed was ~ 24 dB. In addition, a saturation effect is seen above the threshold where the peak received signal did not increase as rapidly as the input power.

Although an explanation of the threshold effect has not yet been found, it has been suggested that background noise could effectively destroy the coherence of the input signal [Helliwell et al., 1980b]. Another possibility is that the feedback mechanism itself has a built-in threshold. Further experiments and theoretical work are needed to answer this question. As illustrated in Figure 4, the threshold power P_t varies with time. Variations in P_t of as much as 10 or 15 dB over a period of half an hour have been observed. These results suggest that the rate of occurrence of growth and triggering from Siple wave injections would increase if the radiated power could be raised. Ultimately we might expect to be able to use measurements of P_t to monitor changes in the flux of energetic particles.

Closely related to triggering is the phenomenon of entrainment. Triggered emissions can be entrained by a Siple pulse whose frequency approaches that of the emission. An example is shown in Figure 5 where a series of falling and rising ramps was transmitted according to the format shown. As can be seen from the responses in the three upper panels, there were several active paths on that day. In the upper two panels the rising ramps produced falling tones at their ends, a case of termination triggering. Each of these falling tones became entrained by the next rising ramp.

Entrainment occurs when the entraining signal and the emission travel in the same duct. Signals traveling in different ducts generally are not coupled to one another, as illustrated in the third panel from the top of Figure 5. Near the end of that panel we see successive triggering and entrainment on the first of two prominent paths. The second path, on the other hand, also shows growth and triggering but the triggered emission crosses the falling tone of the first path without discernable interaction.

Entrainment observations provide an interesting test of the concept of a localized generation region whose position is a function of df/dt. It has been predicted [Helliwell, 1967] that the frequency slope of an emission should be proportional to the displacement of the interaction region from the equator. The relationship of the interaction regions is shown in Figure 6a, while the spectral forms expected from this model are shown in Figure 6b. Entrainment of a natural faller by a natural riser would be in accord with the model. However, one would not expect entrainment of a natural riser by a natural faller. The reason is that the faller travels away from the location of riser generation and hence there could be no interaction between these two signals. Thus a riser entrained by a faller, as sketched in Figure 6b, is a forbidden form according to the model and serves, therefore, as a test of this particular model of natural riser and faller generation.

Although the need for coherence in the input signal for growth and triggering is obvious from the previous examples, there is a curious exception to this requirement. On occasion an amplified narrowband signal from Siple Station is observed to break into a pulsation mode in which sidebands ranging in frequency from 2 to 100 Hz are created. An illustration of the pulsation sideband effect is shown in Figure 7. The two top panels both show

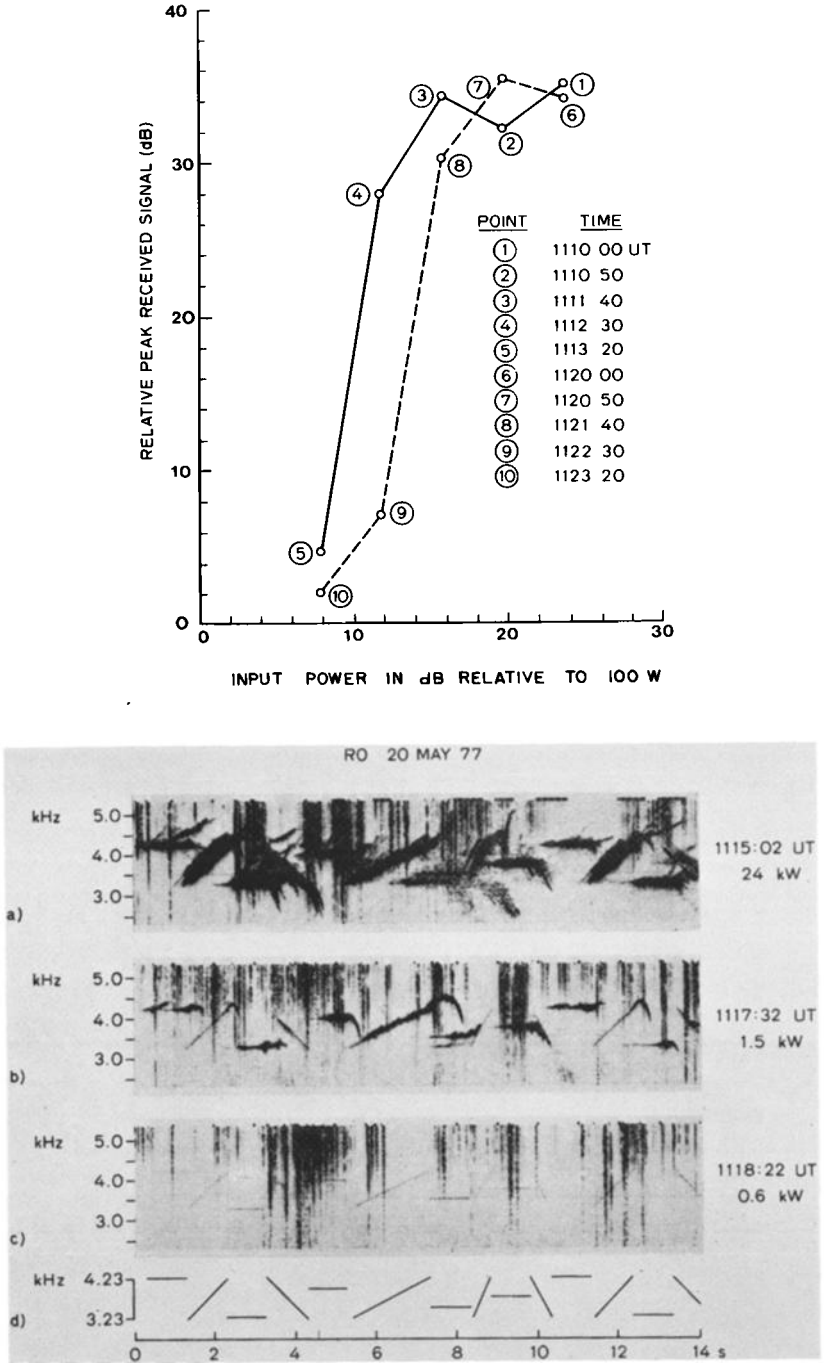

Figure 4. (a) Relative peak perceived power versus input power for two power-step sequences on May 20, 1977. The UT of each measurement is shown in at right. The threshold lies between 8 and 12 s for sequence 1–5 and between 12 and 16 dB for sequences 6–10 [after Helliwell et al., 1980a].

(b) Response of magnetosphere to different transmitter powers, shown at right of each panel. Signal format is shown in lower panel. At 0.6 kW, only one path is evident and there is no growth or triggering. At 1.5 kW a single path shows growth, triggering and weak echoing ($\sim$4.2-s delay). At 24 kW at least four active paths are evident [after Helliwell et al., 1980b].

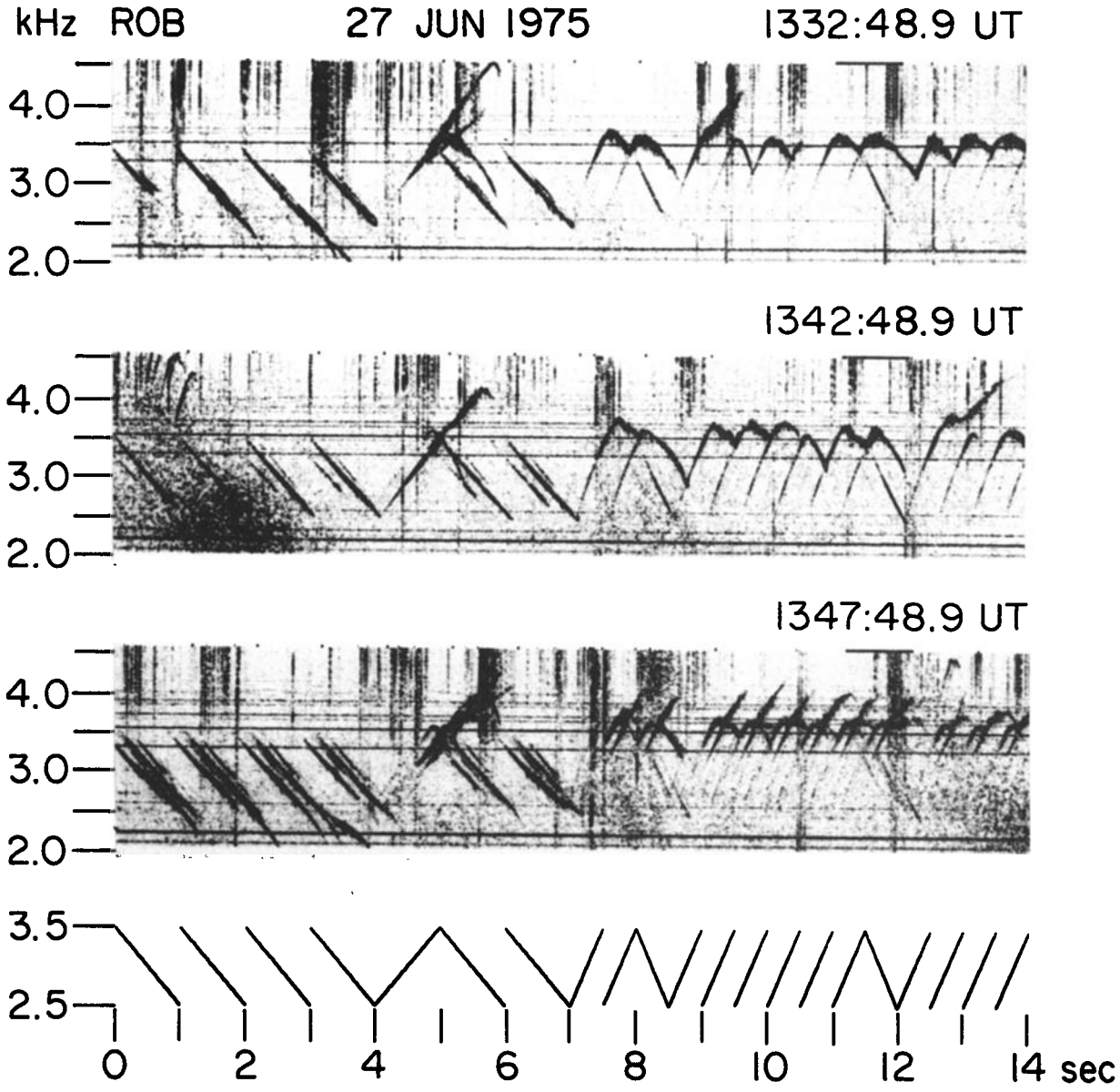

Figure 5. Ramp pulses, whose pattern is shown in the lower panel, trigger inverted hooks that are entrained by the next pulse on the same path. The risers in the 1347:48.9 UT panel appear mainly on two paths. The inverted hooks triggered on the first path cross without interaction with the risers triggered on the second path, proof that the two corresponding interaction regions are uncoupled [after Helliwell and Katsufrakis, 1978].

the same event, in which a signal of constant amplitude and frequency was transmitted from Siple Station. The analyzer resolution was 60 Hz in the top panel and 6 Hz in the second panel, and together they show the fluctuations in frequency and the sideband structure associated with these pulsations. The third and fourth panels show the amplitude measured with filters of 300 Hz and 10 Hz, respectively. We note that the signal reaches saturation without producing significant pulsations and that the appearance of pulsations is independent of whether the carrier intensity is increasing or decreasing. Thus the spectral broadening associated with pulsations does not necessarily affect signal growth as is nearly always the case with similar broadening of the applied signal.

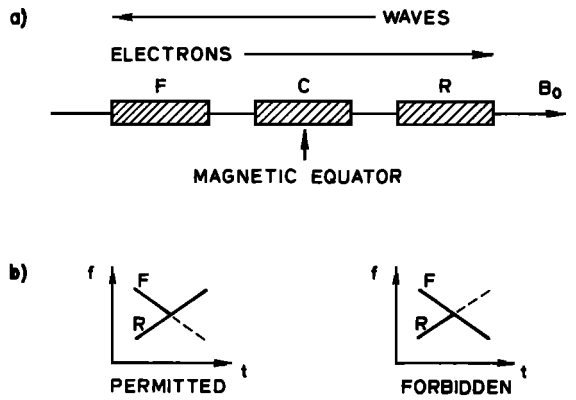

Figure 6. (a) Sketch of postulated relative locations of the interaction regions for constant (C), rising (R), and falling (F) frequency emissions. (b) Corresponding permitted and forbidden entrainment forms. Dashed lines show the trace expected in absence of entrainment.

3. COHERENCE BANDWIDTH

As the results described above have shown, the coherence of the input signal is of primary importance in determining the growth and saturation of the output signal. Thus it is of interest to vary the input spectrum to try to determine the role of coherence in signal amplification. The purpose of this section is to report the preliminary results of an experiment designed to determine the effect of modulation on growth. Three modulation formats were applied to a 1-s pulse transmitted every 2 s, including frequency modulation (F) with unity modulation index, 100% amplitude modulation (A), and beat, or sideband, modulation (S) produced by two equal-amplitude carriers. The carrier amplitudes were approximately the same in each case. Examples of the response to these formats are shown in Figure 8. In each case the modulation frequency is marked and the number 0 applies to zero modulation; that is, a coherent 1-s pulse. As can be seen on the better-defined 0 pulses, the growth rate is of the order of 100 dB. Also, it is clear that when the spacing of the spectral components is 20 Hz the response is very low. For example, with a 20-Hz spacing, the F and A cases at 1209 UT show responses that are only a few decibels above background noise. Although multiple paths are present in these experiments, they must all give about the same variation of intensity with Δf, since otherwise the minimum at 20 Hz would not be sharp.

From these particular records and others from the same run, a curve of maximum output versus modulation frequency was obtained, as shown in Figure 8c. (Similar effects are observed at other frequencies in the VLF range.) We see that for each of the three modulations the output is a minimum at $\Delta f = 20$ Hz. Since 20 Hz is within the range of pulsation frequencies shown in the pulsation experiment, we can understand readily why echoes tend to suppress the growth of freshly injected signals.

It is clear from Figure 8b that as Δf increases above 20 Hz the individual components separate (e.g., A–80 and S–160) and behave more or less independently of one another. However, there is a marked tendency for the lower-frequency component to be weaker than the upper, suggesting suppression by the latter. It must be emphasized that these are preliminary results and that there are features of the experiment that have yet to be described and analyzed before a full interpretation can be attempted.

4. FEEDBACK MODEL

To explain the generation of coherent wave trains, a distributed interaction region has been postulated as shown in Figure 9. Waves travel from right to left, interacting through cyclotron resonance with energetic electrons traveling from left to right. These electrons are shifted in phase relative to the wave by the Lorentz force that acts on each particle [Helliwell and Inan, 1982]. The result is that electrons that initially were randomly phased with respect to the wave became phase-aligned for a brief interval of time (order of 50 ms). During this period the cyclotron radiation from each electron is coherent with the applied wave and may cause wave growth. Furthermore, this radiation tends to peak after the electrons pass through a main wave structure, causing radiation to occur in a region of relatively low field strength, called the 'radiator.' The region of strong field is called the 'buncher.' Given sufficient electron flux the stimulated radiation can exceed the signal level in the buncher. The result is steady growth of the output signal until saturation is reached.

Because of the distributed nature of the feedback loop, some time is required to reach saturation. This is determined by the combination of the particle travel time and the wave group propagation time. For this model it is possible to show that $B = B_0\epsilon^{\gamma t}$, where $\gamma = (G-1)/T$, T is the effective loop delay, and G is the ratio of the stimulated field (B_s) to the output field (B) [Helliwell and Inan, 1982]. For $G > 1$, the system acts as an oscillator. For $G < 1$, oscillation cannot occur and the system is simply an amplifier in which the gain is given by $G_T = 1/(1-G)$.

A sample model calculation of the phase-bunched current for a given applied wave is shown in Figure 10 [Helliwell and Inan, 1982]. Here the full inhomogeneity has been included based on a parabolic approximation of the variation of gyrofrequency with distance from the equator and a diffusive equilibrium model for the background cold plasma. As can be seen, the distance over which the phase between the phase-bunched particles and the wave remains within $\pm\pi/2$ rad is predicted to be $\sim$850 km. This distance is called the interaction length. It is in this region that strong interaction between waves and particles can

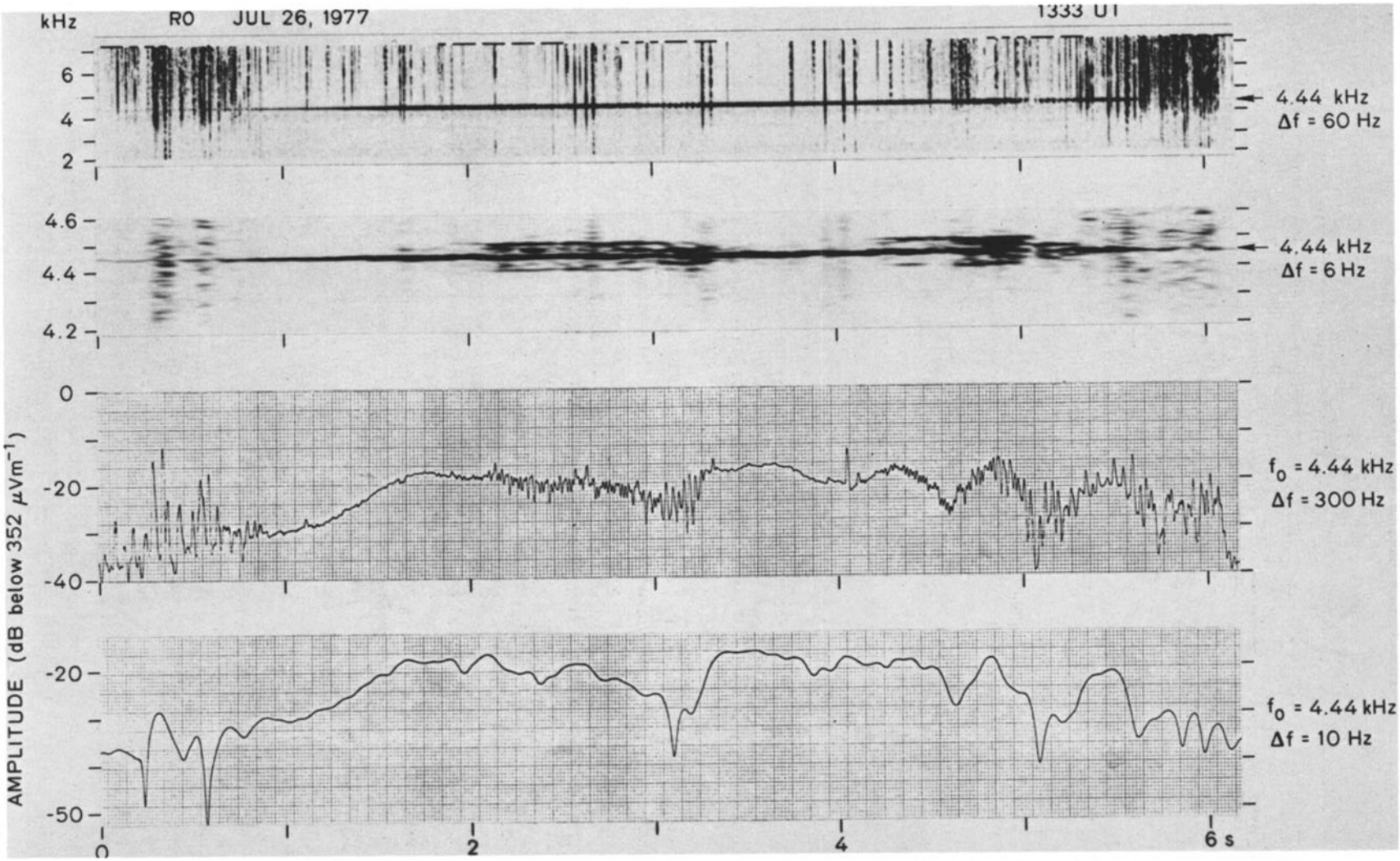

Figure 7. Pulsations generated in the magnetosphere by a constant-frequency, constant-amplitude signal from Siple Station. First and second panels show the spectrum as analyzed with filter bandwidths of 60 and 6 Hz, respectively. The third and fourth panels show the amplitude in bandwidths of 300 and 10 Hz, respectively, centered on the carrier [after Park, 1981].

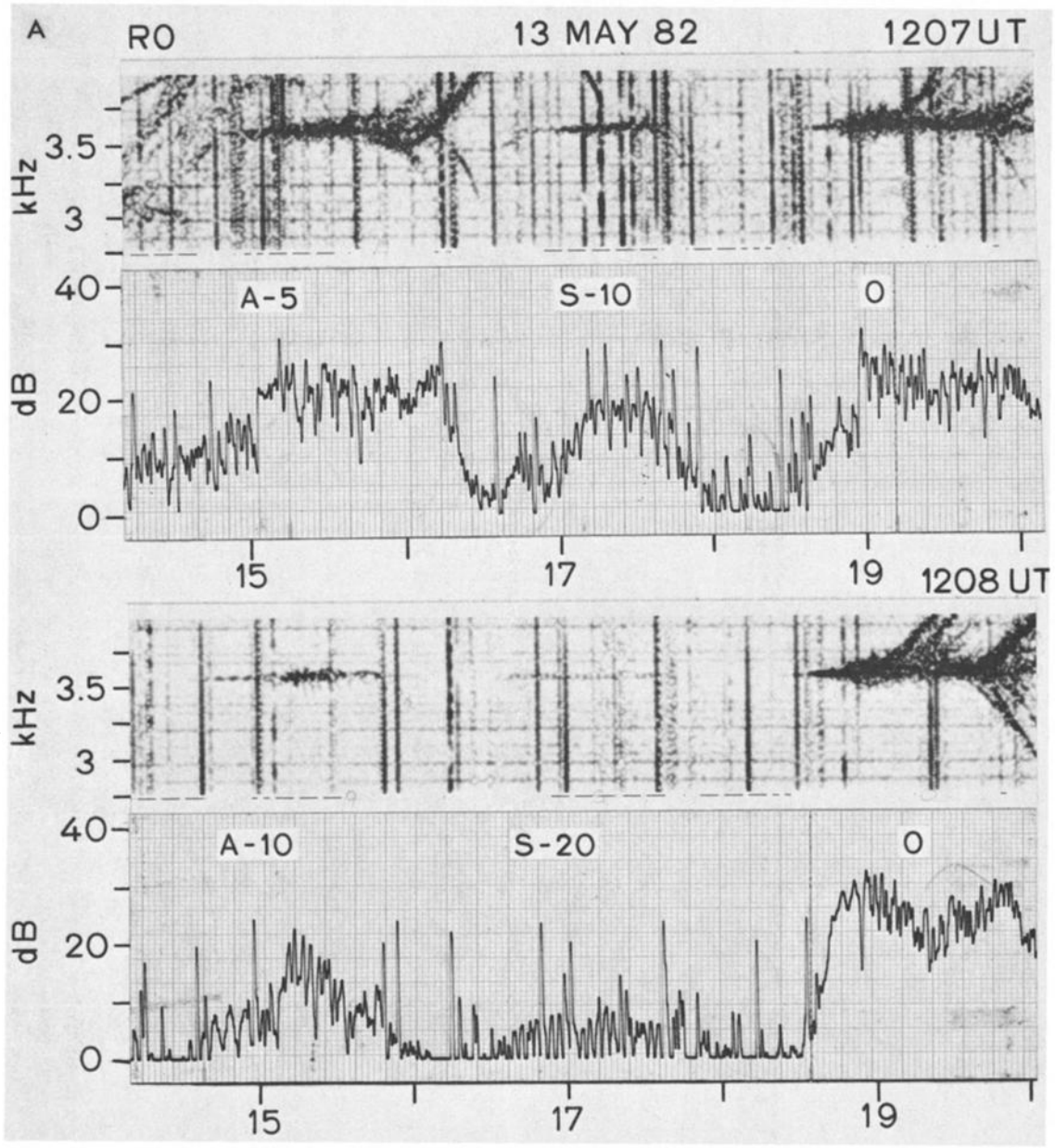

Figure 8. (a, b) Response of magnetosphere to 1-s pulses subject to no modulation (0), 100% amplitude modulation (A), unity-index frequency modulation (F), and sideband modulation (S). Modulation frequency in Hertz is shown for each case. Spectrum is shown in upper panel (12.5-Hz filter bandwidth) and total amplitude in lower panel (300-Hz bandwidth). The received pulses are significantly lengthened because of multipath propagation. (c) Relative output peak field intensity in decibels versus modulation frequency in Hertz. Pluses denote sideband, squares denote amplitude modulation, and triangles frequency modulation.

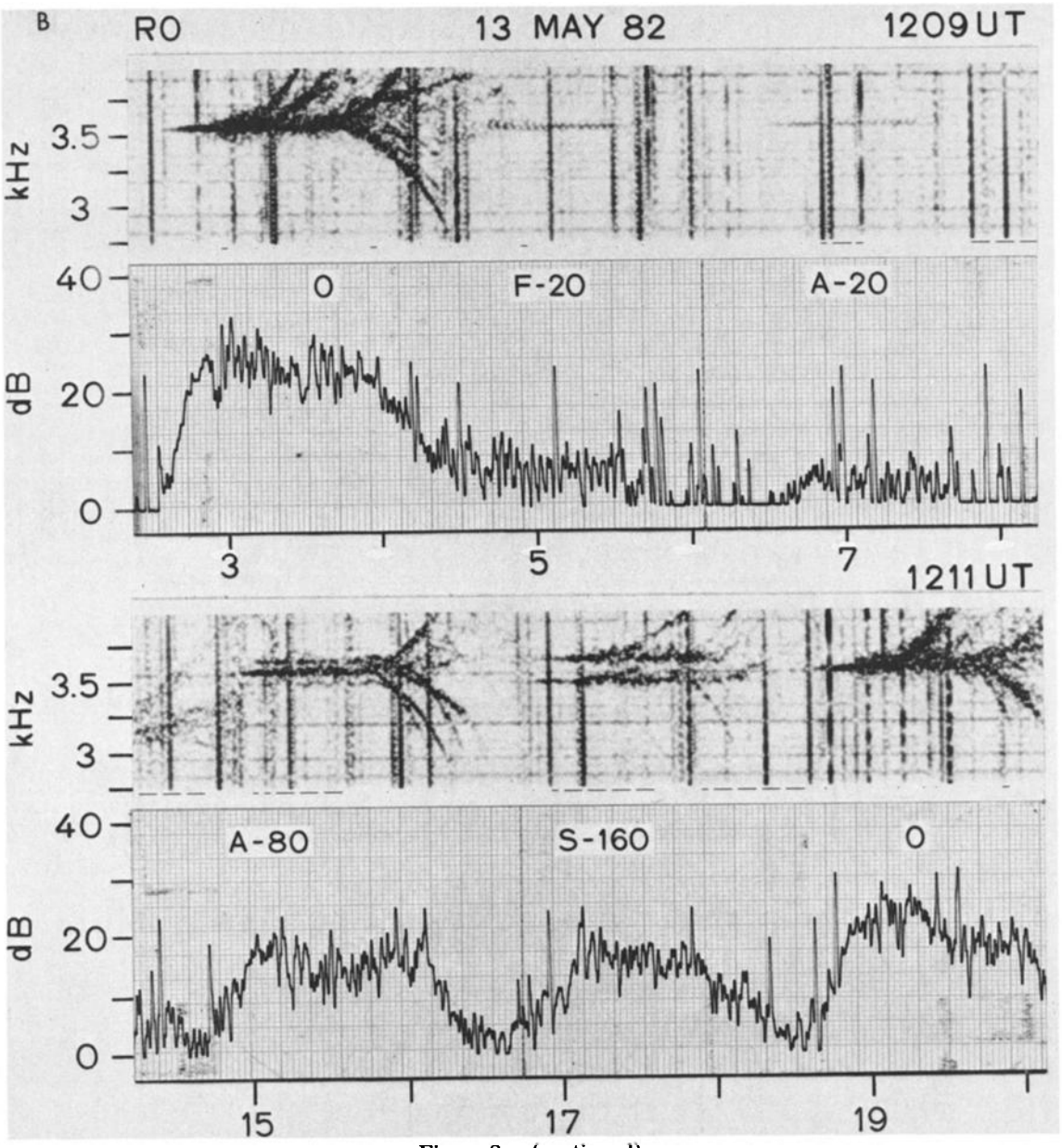

Figure 8. (continued)

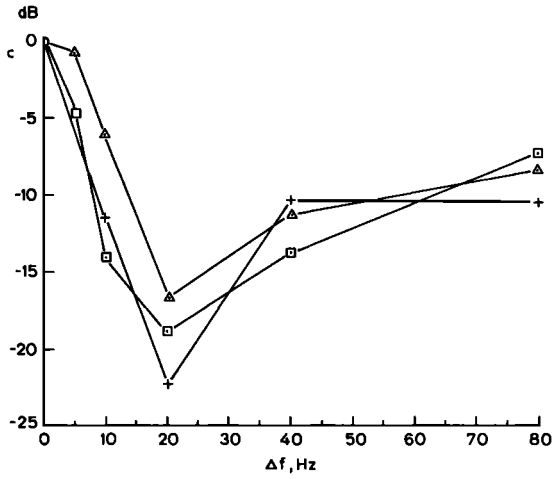

Figure 8. (continued)

take place. As has been shown elsewhere [Helliwell, 1970], for small pitch angles the phase behavior of a sheet of particles with respect to the wave is independent of df/dt. The location of the center of the interaction region accordingly has been called the phase equator [Helliwell and Inan, 1982].

Thus it is possible to analyze the interaction in terms of constant-frequency waves only, using the phase equator concept to describe interactions in which df/dt is not constant. As the magnitude of df/dt increases, the location of the interaction region moves from the magnetic equator either upstream for fallers or downstream for risers (see Figure 6). In either case the gyrofrequency increases, causing the energy of the interacting particles to increase. For the usual electron distribution functions the corresponding flux goes down. Thus under normal conditions one expects a rising or falling ramp to produce less growth than a constant-frequency ramp. These predictions are currently under study using the Siple transmitter. It is interesting to note that the conditions of this experiment are likely to be encountered generally throughout the cosmos. Therefore, the mechanisms involved in the Siple experiments are of universal interest and their understanding should help us to comprehend natural plasmas as well as laboratory plasmas.

5. DISCUSSION AND CONCLUSIONS

We have reviewed the evidence of a new plasma phenomenon which we call the coherent wave instability (CWI). It is characterized by an extremely narrow bandwidth of the order of 0.001 of the frequency of oscillation. We have also

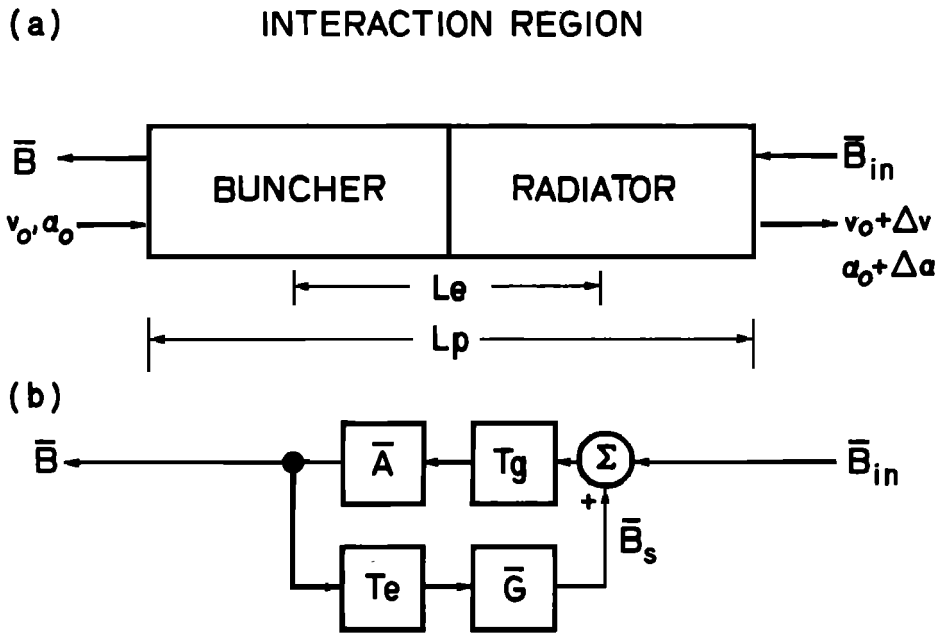

Figure 9. Model of feedback interaction between coherent VLF waves and counter-streaming, cyclotron-resonant electrons. L_p is the interaction length, L_e is the effective length of the feedback loop [after Helliwell and Inan, 1982]. $\mathbf{B}_{in}$ = input signal; $\mathbf{B}$ = output signal; $\mathbf{B}_s = \mathbf{GB}$; v_0 and α_0 = velocity and pitch angle, respectively, of test electrons; T_g = wave group delay; T_e = electron transit time through interaction region; $\mathbf{A}$ = wave propagation factor.

shown that the CWI can be suppressed by a noisy signal having a spectral width of the order of 20 Hz. The CWI shows a threshold, not yet understood, and other interesting effects such as entrainment and quiet band generation. Furthermore, the coherence of the output often breaks down after the signal reaches saturation, giving rise to pulsations in amplitude and frequency, with pulsation frequencies from 2 to 100 Hz. These pulsations are evidence of an additional instability, not yet understood, which occurs with little change in average signal amplitude.

The new results reported in this paper regarding the coherence bandwidth indicate that the minimum response of the magnetosphere is observed when the spacing of the spectral components of the applied signal is ~ 20 Hz. For frequency spacings greater than this, the individual components tend to behave independently although there is considerable interaction between the components up to frequency spacings over 100 Hz. For spacings less than 20 Hz, the spectrum of waves tends to act as a single wave packet with a single response interpreted as a more or less homogeneous group of particles interacting with that wave packet.

An application of the coherent wave instability is in the modification of the radiation belts. Regulation of the intensity of energetic electrons has been attributed to scattering by whistler mode waves [Kennel and Petschek, 1966]. Accordingly, it is important to relate the observed waves to the precipitation of energetic electrons [Inan et al., 1978]. Several experiments have been performed that show one-to-one correlations between triggered emissions and whistlers on the one hand, and ionospheric precipitation effects on the other [Rosenberg et al., 1971; Helliwell et al., 1973, 1980a]. Precipitation effects from the Siple transmitter itself have not yet been clearly identified, probably because the energies of the interacting electrons are too low ($\sim$ 1 keV) to be detected by methods currently employed. Experimentally it has been found that Siple signals seldom produce detectable echoes at Roberval when the equatorial plasma density is less than about 100 cm^{-3}. This corresponds to an electron energy of 20 keV, assuming interaction near the equator at a frequency of 2 kHz. Thus the energies that are normally to be expected in the precipitation flux during the Siple experiments range from ~ 300 eV up to 20 keV. Since height of penetration of electrons in this energy range exceeds 95 km, methods based on D region perturbations (e.g., Trimpi effect) are not particularly useful for this purpose. However, it has been shown in a recent study [Doolittle, 1982] that the lower Fregion should be significantly perturbed by particle fluxes that are affected by the Siple transmitter. Thus it is expected that evidence of precipitation caused by Siple signals will be found through the use of ionosondes and other techniques that are capable of detecting particles in the E and F regions.

Plans for the future call for extending the length (to 43 km) of the antenna at Siple Station so as to increase the power radiated at the lower frequencies, which are expecially well suited to studying precipitation effects. Calculations indicate that doubling the length of the antenna will increase the power radiated at 2.5 kHz by 7 dB. Later it is planned to erect a crossed-dipole antenna to provide for control of the polarization. An additional factor of 2

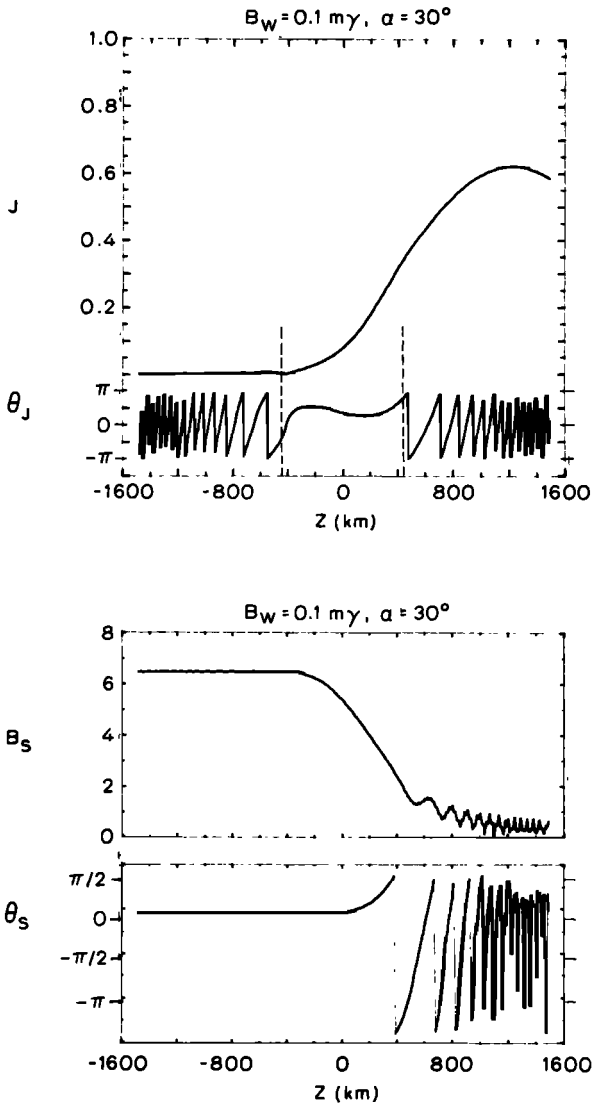

Figure 10. Spatial distributions of the magnitude J and phase θ_J of the stimulated transverse current and the magnitude B_s and phase θ_s of the total stimulated field for $T_r/T_b = 0.197$, an applied signal of 0.1 pT and an electron pitch angle of 30°, where $T_r = L_p/v_{\|}$, $v_{\|}$ = electron parallel velocity, T_b = bunching time [after Helliwell and Inan, 1982].

increase in whistler mode power should be realized when right-hand circular polarization is used. Through these steps it is possible that the Siple signals will exceed the triggering threshold for the low-density regions outside the plasmapause where precipitation effects have been observed in the past. It will then be possible to carry out routine controlled experiments on precipitation as well as on wave growth and wave-wave interaction effects of the kind described in this paper.

Acknowledgments. This work was supported by the National Science Foundation under grants DPP80-22282 and DPP80-22540 under the Division of Polar Programs. The final manuscript was prepared by K. Dean.

REFERENCES

Arnoldy, R. L., L. S. Cahill, Jr., S. B. Mende, and R. Risler, ULF-associated particle precipitation at Siple Station, *Antarct. J., XVI* (5), 209, 1981.

Doolittle, J. H., Modification of the ionosphere by VLF wave-induced electron precipitation, *Tech. Rep. E4-21301218*, Radiosci. Lab., Stanford Electron. Labs., Stanford Univ., Stanford, Calif. 94305.

Helliwell, R. A., A theory of discrete VLF emissions from the magnetosphere, *J. Geophys. Res., 72*, 4773. 1967.

Helliwell, R. A., Intensity of discrete VLF emissions, in *Particles and Fields in the Magnetosphere*, edited by B. M. McCormac, 292, D. Reidel, Dordrecht, 1970.

Helliwell, R. A., and U. S. Inan, VLF wave growth and discrete emission triggering in the magnetosphere: A feedback model, *J. Geophys. Res., 87*, 3537, 1982.

Helliwell, R. A., and J. P. Katsufrakis, Controlled wave-particle interaction experiments, in *Upper Atmosphere Research in Antarctica, Antarct. Res. Ser.* vol. 29, edited by L. J. Lanzerotti and C. G. Park, 100, AGU, Washington, D. C., 1978.

Helliwell, R. A., J. P. Katsufrakis, and M. L. Trimpi, Whistler-induced amplitude perturbation in VLF propagation, *J. Geophys. Res., 78*, 4649, 1973.

Helliwell, R. A., S. B. Mende, J. H. Doolittle, W. C. Armstrong, and D. L. Carpenter, Correlations between λ4278 optical emissions and VLF wave events observed at L ~ 4 in the Antarctic, *J. Geophys. Res., 85*, 3376, 1980a.

Helliwell, R. A., D. L. Carpenter, and T. R. Miller, Power threshold for growth of coherent VLF signals in the magnetosphere, *J. Geophys. Res., 85*, 3360, 1980b.

Inan, U. S., T. F. Bell, and R. A. Helliwell, Nonlinear pitch angle scattering of energetic electrons by coherent VLF waves in the magnetosphere, *J. Geophys. Res., 83*, 3235, 1978.

Kennel, C. F., and H. E. Petschek, Limit on stably trapped particle fluxes, *J. Geophys. Res., 71*, 1, 1966.

Lanzerotti, L. J., Studies of geomagnetic pulsations, in *Upper Atmosphere Research in Antarctica, Antarct. Res. Ser.* vol. 29, edited by L. J. Lanzerotti and C. G. Park, 130, AGU, Washington, D. C., 1978.

Matthews, D. L., Siple Station magnetospheric physics campaign, *Antarct. J., XVI* (5), 202, 1981.

Mende, S. B., R. L. Arnoldy, L. J. Cahill, Jr., J. H. Doolittle, W. C. Armstrong, and A. C. Fraser-Smith, Correlations between λ4278-Å optical emissions and a Pc 1 pearl event observed at Siple Station, *J. Geophys. Res., 85*, 1194, 1980.

Park, C. G., Generation of whistler-mode sidebands in the magnetosphere, *J. Geophys. Res., 86*, 2286, 1981.

Park, C. G., and D. L. Carpenter, Very low frequency radio waves in the magnetosphere, in *Upper Atmosphere Research in Antarctica, Antarct. Res. Ser.* vol. 29, edited by L. J. Lanzerotti and C. G. Park, 72, AGU, Washington, D. C., 1978.

Raghuram, R., R. L. Smith, and T. F. Bell, VLF Antarctic antenna: Impedance and efficiency, *IEEE Trans. on Antennas and Propag., AP-22*, 334, 1974.

Raghuram, R., T. F. Bell, R. A. Helliwell, and J. P. Katsufrakis, Quiet band produced by VLF transmitter signals in the magnetosphere, *Geophys. Res. Lett., 4*, 199, 1977.

Rosenberg, T. J., and J. R. Barcus, Energetic particle precipitation from the magnetosphere, in *Upper Atmosphere Research in Antarctica, Antarct. Res. Ser.* vol. 29, edited by L. J. Lanzerotti and C. G. Park, 42, AGU, Washington, D. C., 1978.

Rosenberg, T. J., R. A. Helliwell, and J. P. Katsufrakis, Electron precipitation associated with discrete very-low-frequency emissions, *J. Geophys. Res., 76*, 8445, 1971.

Stiles, G. S., and R. A. Helliwell, Stimulated growth of coherent VLF waves in the magnetosphere, *J. Geophys. Res., 82*, 523, 1977.